Supplemental Information

Manipulation and Capture of Aβ Amyloid Fibrils and Monomers by DC Insulator Gradient Dielectrophoresis (DC-iGDEP)

Sarah J. R. Staton[a,b], Paul V. Jones[a], Ginger Ku[c], S. Douglass Gilman[d], Indu Kheterpal[c], and Mark A. Hayes[a]*

[a] Department of Chemistry and Biochemistry, Arizona State University, Tempe, AZ 85286 USA, [b] Currently at Naval Research Laboratory, Washington, DC 20375, [c] Pennington Biomedical Research Center, Louisiana State University System, Baton Rouge, LA, 70808, USA, [d] Department of Chemistry, Louisiana State University, Baton Rouge, LA, 70803, USA

Table of Contents

A) Details of DC-iGDEP Device Fabrication

The DC-iGDEP devices were fabricated utilizing standard photolithography, fabrication, and bonding techniques.[1] Photomasks were designed in AutoCAD (Autodesk; San Rafael, CA, USA), and photolithographic positive stamps were made using AZ P4620 photoresist (AZ Electronic Materials; Branchburg, NJ, USA) and contrast enhancement material CEM388SS (Shin-Etsu MicroSi; Phoenix, AZ, USA). Device channels were fabricated from polydimethylsiloxane (PDMS) with a microscope slide coverplate. The PDMS channels were cast using Sylgard 184 silicone elastomer kit PDMS (Dow/Corning; Midland, MI, USA). Shortly after the PDMS portion of the device was fabricated, access holes were made using a hole punch (3 mm diameter through 0.5–1 cm of PDMS), and then the PDMS portion of the device was sealed to the glass cover plate by plasma oxidation followed by contact sealing.[2] The geometry of the separatory portion of the DC-iGDEP channel consisted of successive triangular units that extended into the open volume to induce local electric field gradients. The insulating PDMS 60º triangles began with a base length of 6 μm and a height of 5.2 μm. Their side length and width increased by 40 μm after every six repeats (Fig. 1, main text), resulting in an initial gap distance of 945 μm and a

final gap distance of 27 µm. The separatory portion of the DC-iGDEP channel connected the two reservoirs created by the hole punch, where sample and buffer were introduced into the channel. The channel depth ranged from 13 to 16 µm.

Sample was introduced via the reservoir at the end of the channel with the larger gap distance. After sample introduction, platinum wire electrodes (0.404 mm diameter, 99.9% purity; Alfa Aesar; Ward Hill, MA, USA) were placed in each of the reservoirs in contact with the solution and attached to a power supply (Series 225, Bertram). The voltage was applied at a potential between 0 and 1000 V, for 1-15 min depending upon the experiment. Visualization was achieved using an Olympus inverted IX70 microscope with a mercury short arc H30 103 w/2 light source from OSRAM and an Olympus DAPI, FITC, Texas Red triple band pass cube (Olympus; Center Valley, PA, USA).

Videos and still images were collected with a monochrome QICAM cooled CCD camera (QImaging, Inc.; Surrey, BC, Canada) and Streampix III image capture software (Norpix, Inc.; Montreal, QC, Canada). The fluorescence intensity was then analyzed with ImageJ (NIH; Bethesda, MD). Three different regions of interest (ROI) were selected (Fig. S1). The ROIs represent the capture zone (gate), a background area within the channel (recess), and a background outside of the channel (PDMS). Table ESI-1 uses the same ROIs described in Fig. ESI-1. The data presented in Table 1 represent multiple replicates (n>3) with isolation events occurring in the same position. Ratios of the various ROIs were utilized to determine enrichment of fluorescent fibrils in the capture zone when compared to the rest of the microfluidic channel filled with sample as well as a background of the device outside of the channel. Each ROI represents equally sized areas.

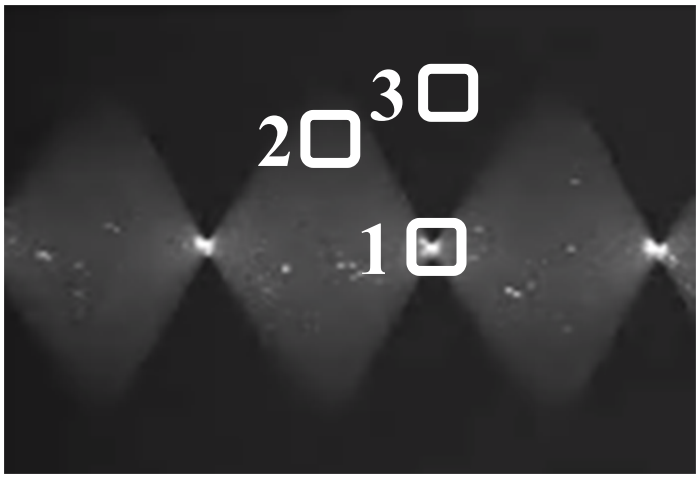

Fig. ESI-1: Regions of interest (ROIs) indicated as described in the text. Three different areas were selected to determine the enrichment of fibril concentration in the capture zone using the fluorescence intensities in each region. The areas depicted here are larger than the actual ROIs used for ease of viewing.

Table ESI-1: Fluorescence Intensity Values in ROIs for Fibril Samples.

400 V				
	Photo label	**Intensity/Area**		
Gate	1	212.8		**Ratio**
Recess	2	52.2	**Gate/Recess**	4.1
PDMS	3	35.9	**Gate/PDMS**	5.9

600 V				
	Photo label	**Intensity/Area**		
Gate	1	207.0		**Ratio**
Recess	2	40.0	**Gate/Recess**	5.2
PDMS	3	36.1	**Gate/PDMS**	5.7

800 V				
	Photo label	**Intensity/Area**		
Gate	1	214.5		**Ratio**
Recess	2	60.0	**Gate/Recess**	3.6
PDMS	3	36.1	**Gate/PDMS**	5.9

1000 V				
	Photo label	**Intensity/Area**		
Gate	1	211.7		**Ratio**
Recess	2	61.2	**Gate/Recess**	3.5
PDMS	3	36.1	**Gate/PDMS**	5.9

B) Preparation of Aβ (1-40) Monomers and Fibrils

Both Aβ (1-40) monomer and fibril samples were prepared as described in detail previously.[3-5] Briefly, Aβ (1-40) peptide (W.M Keck Foundation Biotechnology Research Laboratory, Yale University; New Haven, CT) and carboxyfluorescein (FAM) labeled Aβ (1-40) peptide (Anaspec Inc.; Fremont, CA) were first treated with trifluoroacetic acid (TFA) and hexafluoroisopropanol (HFIP) to remove any preexisting aggregates. For Aβ monomer samples, the solvent was evaporated off, and the peptides were dissolved in 10.00 mM Tris at pH 7.79. FAM-Aβ (1-40) monomer was mixed with Aβ (1-40) monomer at a mass ratio of 1:4. The total Aβ concentration of the monomer solution was determined to be 30 μM using a Shimadzu HPLC-UV instrument with detection at 215 nm as described previously.[3-5]

For the Aβ (1-40) fibril samples, TFA was evaporated off, and the peptides were dissolved in HFIP. The concentration of each peptide was determined using HPLC-UV. FAM-Aβ (1-40) monomer was mixed at a mass ratio of 1:4 with Aβ (1-40) monomer. HFIP was evaporated off, and the peptide mixture was dissolved stepwise in equal volumes of 2.0 mM NaOH and 2X phosphate buffered saline (PBS) containing 22.8 mM phosphate, 274 mM NaCl, 5.4 mM KCl and 0.1% NaN_3 at pH 7.4. The samples were centrifuged at 50,000 g for a minimum of 10 h at 4 °C. Fibril formation was initiated by addition of a small quantity (0.1% by weight of total Aβ monomer) of fibrillar aggregates to the supernatant from a previous fibril synthesis. The mixture was then incubated at 37 °C for 7 d. Depletion in monomer during fibril formation was monitored using HPLC-UV with detection at 215 nm as described previously.[3-5] Fibril growth was monitored using ThT fluorescence until complete (5-7 days), and the quality of fibrils was assessed by electon microscopy. For direct comparison with Aβ (1-40) monomer samples in DC-iGDEP analysis, fibril samples were buffer exchanged from PBS to 10.00 mM Tris electrophoresis buffer at pH 7.79.[6] The monomer-equivalent concentrations of all samples were determined to be 30 μM by HPLC-UV.

C) COMSOL Mathematical Modeling

In order to aid in understanding and interpreting particle behavior within the sawtooth-patterned microchannel, the electric field distribution within the microdevice was determined numerically and plotted. This was accomplished using finite element analysis software COMSOL Multiphysics 4.1 (COMSOL, Inc., Burlington, MA) in the "conductive media DC" mode. Models created in this mode are time-independent calculations of field strength within an aqueous medium. COMSOL computes the electric field by solving the Laplace equation, $\nabla^2 (\varphi) = 0$, for potential distribution at various points throughout the channel, along a predefined mesh. The boundary conditions are defined as distinct potentials at the channel inlet and outlet and electrical insulators at the channel walls.

A properly scaled model of the main channel geometry was produced and imported into the COMSOL environment. In order to simplify the model, a 2D approximation of the channel was utilized. Due to the placement of electrodes in distant reservoirs and the high width to depth ratio of the channel, the effects of channel depth on electrical potential were neglected. The effects of particles on the electric field distribution were also neglected.

Reservoir-channel junctions were set to predetermined potentials similar to those used during experiments. V_{inlet} and V_{outlet} were 0 V and -550 V, respectively. All other boundaries (representing PDMS and glass walls) were set to be perfect insulators; an approximation justified by the large difference in conductivity between the fluid medium and the channel walls. The conductivity and relative

permittivity of the medium were set at 1.2 S/m and 78, respectively. This conductivity is consistent with values that can be obtained using standard phosphate-buffered saline.

A triangular mesh was applied to the entire channel area. The mesh contained approximately 97,000 triangular elements and 680 vertex elements. Through finite element analysis, the software approximates the electric potential at each mesh point. From these numerical values other useful parameters relevant to electrokinesis and dielectrophoresis may be determined, such as electric field strength, $|E|$, and the gradient of square of the electric field, $\nabla|E|^2$. Built-in tools enable graphic representation of the resulting data.

Since dielectrophoretic force is proportional to $\nabla|E|^2$, the magnitude of this term along the channel centerline was extracted from the COMSOL model using a 2D cut line. Localized maxima from this dataset correspond to channel constrictions or gates along the sawtooth pattern. When these values of $\nabla|E|^2$ are plotted as a function of gate width, the relationship can be reasonably approximated with a power function (Fig. ESI-2). Visualizing the data in this manner illustrates the rapid scaling of dielectrophoretic force with increasing geometric constriction of the channel.

Amongst other things, dielectrophoretic force is proportional to particle size. Thus, capture of

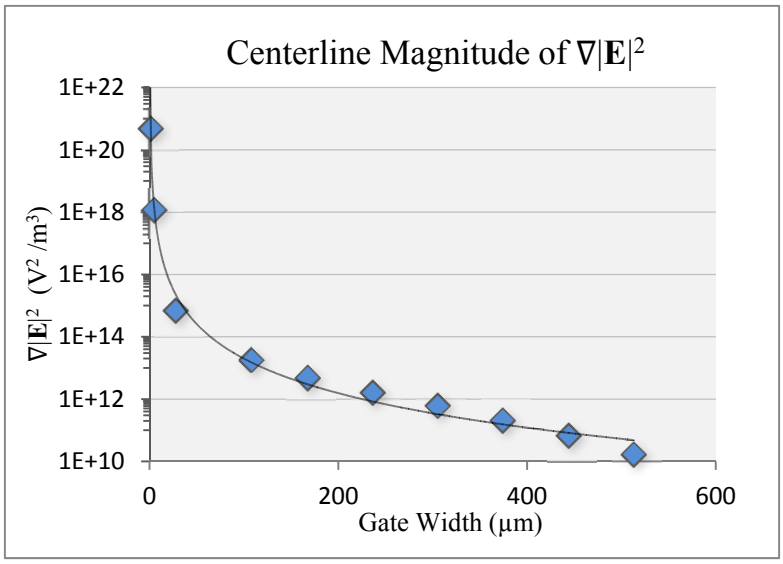

Fig. ESI-2 Plot showing computed magnitudes of $\nabla|E|^2$ along the microchannel centerline versus gate width. Vertical axis is plotted using a logarithmic scale. The trend line shows that the relationship between data points can be approximated using a power function.

smaller particles such as protein monomers will require larger values of $\nabla|E|^2$. Fig. ESI-2 illustrates that drastically larger values of $\nabla|E|^2$ are attainable by increasing the constriction ratio at gates. Using the following assumptions and the $\nabla|E|^2$ values determined in Fig. ESI-2, it was found that a gate width of ~10 nm would be sufficient to capture Aβ monomers. The assumptions used in the calculation were that there was negligible electroosmotic flow, the Aβ monomer is spherical with a diameter of ~2.5 nm, the monomer μ_{EP} is 1.2 x10^{-4} $cm^2/(Vs)$, the viscosity and permittivity of the medium are similar to that of water, and the conductivity of the Aβ monomer is significantly less than that of the fluid medium.

D) References

1. C. Mack, *Fundamental Principles of Optical Lithography: The Science of Microfabrication*, Wiley, Hoboken, 2008.
2. K. Haubert, T. Drier and D. Beebe, *Lab Chip*, 2006, **6**, 1548-1549.
3. R. Picou, J. P. Moses, A. D. Wellman, I. Kheterpal and S. D. Gilman, *Analyst*, 2010, **135**, 1631-1635.
4. R. A. Picou, I. Kheterpal, A. D. Wellman, M. Minnamreddy, G. Ku and S. D. Gilman, *J Chromatogr. B*, 2011, **879**, 627-632.
5. B. O'Nuallain, A. K. Thakur, A. D. Williams, A. M. Bhattacharyya, S. Chen, G. Thiagarajan and R. Wetzel, in *Methods Enzymol*. 2006, **413,** 34-74.
6. I. Kheterpal, S. Zhou, K. D. Cook and R. Wetzel, *Proc. Natl. Acad. Sci. USA*, 2000, **97**, 13597-13601.